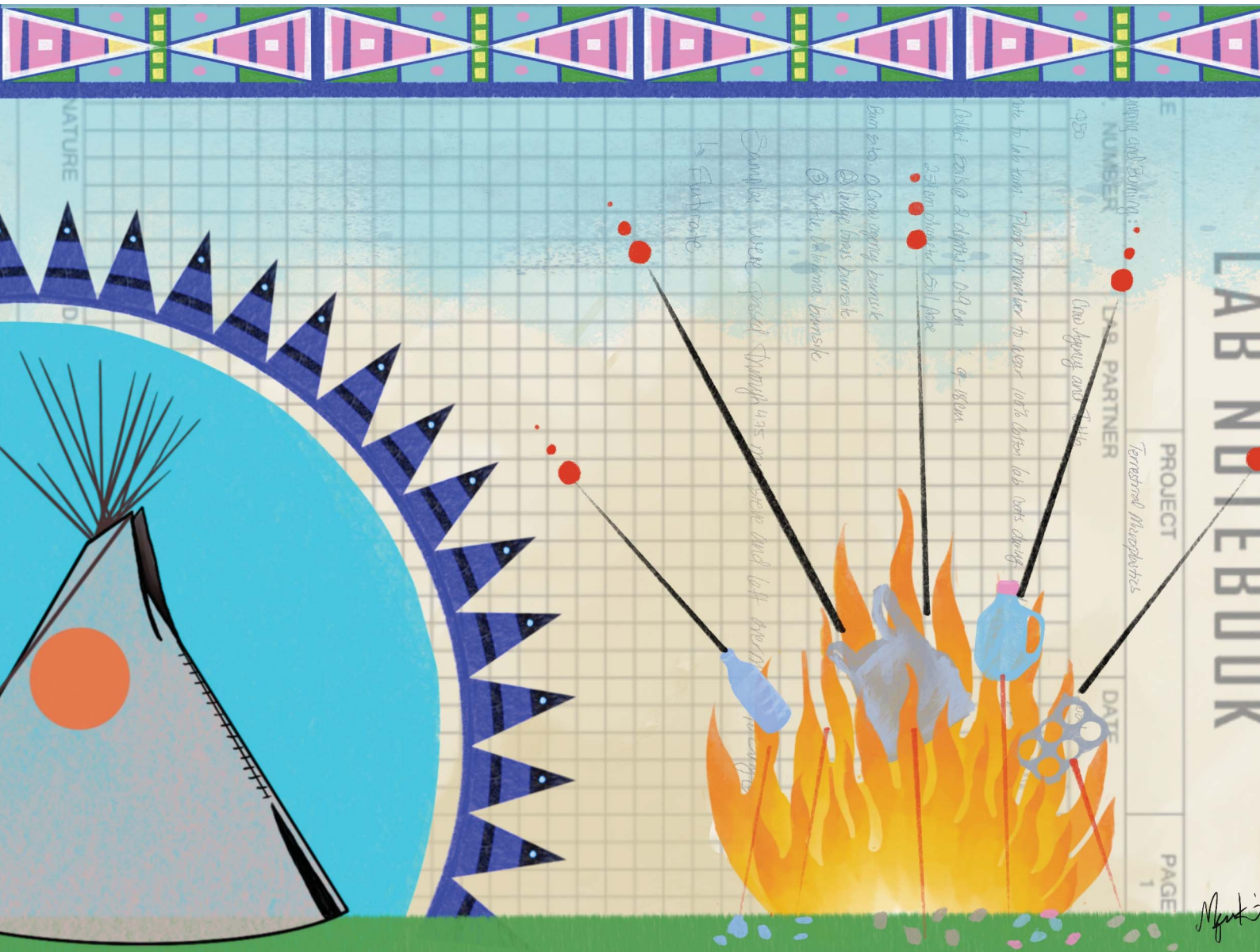


# Environmental Science Processes & Impacts

rsc.li/espi



ISSN 2050-7887

## PAPER

Jorge Gonzalez-Estrella *et al.*

Emerging investigator series: open dumping and burning: an overlooked source of terrestrial microplastics in underserved communities



Cite this: *Environ. Sci.: Processes Impacts*, 2025, 27, 52

## Emerging investigator series: open dumping and burning: an overlooked source of terrestrial microplastics in underserved communities†

Kendra Z. Hess, <sup>a</sup> Kyle R. Forsythe, <sup>a</sup> Xuewen Wang, <sup>a</sup> Andrea Arredondo-Navarro, <sup>a</sup> Gwen Tipling, <sup>a</sup> Jesse Jones, <sup>a</sup> Melissa Mata, <sup>a</sup> Victoria Hughes, <sup>a</sup> Christine Martin, <sup>b</sup> John Doyle, <sup>b</sup> Justin Scott, <sup>a</sup> Matteo Minghetti, <sup>c</sup> Andrea Jilling, <sup>d</sup> José M. Cerrato, <sup>e</sup> Eliane El Hayek <sup>f</sup> and Jorge Gonzalez-Estrella <sup>\*a</sup>

Open dumping and burning of solid waste are widely practiced in underserved communities lacking access to solid waste management facilities; however, the generation of microplastics from these sites has been overlooked. We report elevated concentrations of microplastics (MPs) in soil of three solid waste open dump and burn sites: a single-family site in Tuttle, Oklahoma, USA, and two community-wide sites in Crow Agency and Lodge Grass, Montana, USA. We extracted, quantified, and characterized MPs from two soil depths (0–9 cm and 9–18 cm). The average of abundance of particles found at community-wide sites three sites (18, 460 particles kg<sup>-1</sup> soil) equals or exceeds reported concentrations from currently understood sources of MPs including biosolids application and other agricultural practices. Attenuated total reflectance Fourier transformed infrared (ATR-FTIR) identified polyethylene as the dominant polymer across all sites (46.2–84.8%). We also detected rayon (≤11.5%), polystyrene (up to 11.5%), polyethylene terephthalate (≤5.1), polyvinyl chloride (≤4.4%), polyester (≤3.1), and acrylic (≤2.2%). Burned MPs accounted for 76.3 to 96.9% of the MPs found in both community wide dumping sites. These results indicate that solid waste dumping and burning activities are a major source of thermally oxidized MPs for the surrounding terrestrial environment with potential to negatively affect underserved communities.

Received 19th July 2024  
Accepted 11th October 2024

DOI: 10.1039/d4em00439f  
rsc.li/espi

### Environmental significance

Our work determined the quantity and vertical distribution of microplastics (MPs) in soil surrounding open dumping and burning sites. This work unveils the abundance of MPs in the terrestrial environment around open dumping and open burning sites near underserved communities. Generation of MPs through open dumping and burning of solid waste is an issue concerning not only our partner communities for this study in Oklahoma and Montana, but also globally, and has profound environmental implications for rural and urban underserved communities worldwide.

## 1 Introduction

Human activities generated about 242 million metric tons of solid waste in 2016 according to the World Bank.<sup>1</sup> Plastic waste represents about 12.2% of the solid waste of the United States of America (US)<sup>2</sup> and 12% around the world.<sup>1</sup> In the specific case of the US, such estimation disregards rubber or synthetic polymer based textiles as part of the plastic waste as these wastes are grouped under the rubber, leather, and textiles category.<sup>2</sup>

Waste disposal practices are a function of each country's economy.<sup>1,3</sup> In high income countries, most of the waste is either landfilled (39% of the total waste), recycled (29%), or incinerated (22%). Low income countries, on the other hand, dispose about 93% of their waste in open dump sites.<sup>1</sup> Open

<sup>a</sup>School of Civil & Environmental Engineering, Oklahoma State University, 248 Engineering North, Stillwater 74078, Oklahoma, USA. E-mail: jorgego@okstate.edu

<sup>b</sup>Little Bighorn College, Crow Agency, MT 59022, USA

<sup>c</sup>Department of Integrative Biology, Oklahoma State University, Stillwater 74078, Oklahoma, USA

<sup>d</sup>Department of Environmental Health Sciences, University of South Carolina, Columbia, SC 29201, USA

<sup>e</sup>Gerald May Department of Civil, Construction & Environmental Engineering, University of New Mexico, MSC01 1070, Albuquerque, New Mexico 87131, USA

<sup>f</sup>Department of Pharmaceutical Sciences, University of New Mexico, College of Pharmacy, MSC09 5360, Albuquerque, New Mexico, 87131, USA

† Electronic supplementary information (ESI) available. See DOI: <https://doi.org/10.1039/d4em00439f>



dumping is also prevalent in isolated and unserved communities even in upper middle- and high-income countries.

In the US, some rural communities and isolated Native American Tribes lack access to waste collection services and management facilities and, as a result, rely upon open burning to dispose of solid waste.<sup>3,4</sup> About 18–29 million metric tons of plastic waste was burned in 2016.<sup>3,5</sup> Though burning solid waste disposed in open pits may reduce waste volume, pathogen exposure,<sup>3</sup> and undesirable odor, the sites lack protective barriers and result in refuse placed directly above the ground.<sup>6</sup> Open dumping and burning of solid waste are well-known sources of suspended particulate matter, odorous compounds, and leachates among other pollutants.<sup>3,7</sup>

Open dumping and burning sites are also an unexplored source of terrestrial microplastics (MPs, plastic pieces with a size between 1  $\mu\text{m}$  and 5 mm).<sup>8</sup> It is likely that open burning sites generate MPs due to the lack of temperatures that are sufficient or consistent enough to incinerate plastic waste, which represents between 6.4 and 13% of the solid waste.<sup>1</sup> Partially-combusted plastics generated from these burning processes have more potential to generate MPs relative to non-oxidized plastics. Other types of oxidized MPs (e.g., UV oxidized) have shown increased toxicity,<sup>9</sup> sorption capacity,<sup>10,11</sup> brittleness,<sup>12</sup> and leaching capacity of additives<sup>13–15</sup> among other effects. This highlights the importance of considering not only MP quantity and plastic type, but also the MP functional and surface chemistry.<sup>16,17</sup>

Compared to aquatic ecosystems, the current understanding of sources and levels of MP pollution in terrestrial ecosystems is limited.<sup>18–21</sup> Common sources of MPs in soils include improper disposal of domestic and industrial waste, urban and rural runoff, wet and dry deposition, and biosolids.<sup>22,23</sup> However, even less research has been conducted to understand the abundance and type of MPs in soils due to open dumping and burning of solid waste, which is a common waste disposal practice in underserved rural communities.<sup>1,3,24–27</sup> Thus far, these few studies agree on microplastic occurrence<sup>28,29</sup> in a range of 50 to 1110 items  $\text{kg}^{-1}$ .<sup>30</sup>

Our work determined the abundance and vertical distribution of MPs in soil surrounding open dumping and burning sites at a single-family open burning site located in Tuttle, Oklahoma (Tuttle burn site), and two Native American community-wide sites in Crow Agency, Montana (Crow Agency burn site and Lodge Grass dump site). We identified the polymer type and functional chemistry of MPs and trends in MPs abundance, polymer size, and surface chemistry in relation to soil physiochemical characteristics, depth, and site history and use. Few studies have examined the occurrence of MPs in waste disposal sites, and even fewer have considered the surrounding soils.<sup>3,4,27–30</sup> Microplastics generated from open burning sites likely show different oxidation patterns than other MPs found in the environment that have been generated from other weathering processes. Our study assesses the abundance of MPs near open dumping and open burning sites in underserved communities and analyzes the functional chemistry of MPs with a thermal oxidation signature; and it highlights the importance of understanding MP contamination affecting

underserved communities which are frequently overlooked in mainstream science.

## 2 Methods

### 2.1 Quality assurance and quality control

To reduce MP contamination during laboratory procedures, all glassware was sonicated for 30 min in deionized (DI) water and covered with aluminum foil until use. All procedures except for elutriation and fluorescence microscopy were conducted in a designated MP laboratory which had extra air filtration units and regular rigorous cleaning of surfaces. All applicable procedures were conducted in a laminar flow fume hood. Lab coats made of 100% cotton were worn during all laboratory procedures and synthetic clothing was avoided as much as possible during sampling. A triplicate laboratory control was conducted to detect lab-based contamination. To account for base-level environmental MP contamination, background samples were collected and run in triplicate. The background for the Tuttle burn site was a field in nearby Stillwater, OK, and the background for Crow Agency burn site and Lodge Grass dump site was adjacent ranch land. No prior dumping or burning was reported in any of these background sites.

### 2.2 Site characterization and sample collection

Faculty of Little Big Horn Community College, Crow Agency, MT, identified 'Crow Agency burn site' and 'Lodge Grass dump site', which serve approximately 2000 and 440 people, respectively. Homeowners of Tuttle, OK, identified the burn site which serves two people. Faculty and the homeowners described current solid waste management practices. The approximate area of each site was determined using Google Earth. The area of the Tuttle burn site was approximately 50  $\text{m}^2$ . The areas of the Crow Agency burn site and Lodge Grass dump site were approximately 32 200  $\text{m}^2$  and 36 000  $\text{m}^2$ , respectively (Table S1†). Aerial images and sampling coordinates are available in Fig. S1 and Table S3.† Partners from Little Big Horn Community College reported that solid waste burning occurred regularly at the Tuttle burn site and Crow Agency burn site, while primarily dumping without burning occurred at Lodge Grass dump site. The Tuttle burn site has been in use for about 30 years, while Crow Agency burn site and Lodge Grass dump site began only about 2 years prior to the sampling date.

The trash piles were not homogenous; thus, sites were divided into quadrants (based on cardinal directions) to account for variation in soil or MP characteristics. Samples were collected in a randomized design, and samples were taken with two different purposes: (1) we collected a bulk sample to  $\sim 18$  cm in depth using a shovel to determine texture and organic matter content; and (2) we collected soil from  $\sim 0$  to 9 and 9 to 18 cm depths using a 2.54 cm diameter soil probe to evaluate MP size and content distribution. Bulk and core samples were taken from the same quadrants. Approximations in sample depth were due to varied compaction levels across the sampling areas which at times physically limited the depth to which the probe could be driven into the soil. Three sampling locations were selected randomly within each quadrant of the pile. Subsamples



were collected from each location and combined to obtain approximately  $\sim 1$  kg of soil per composite sample, providing four replicate soil samples per site. Samples were collected in 3.78 L new and clean plastic sealable bags to retain moisture during transport and were refrigerated upon arrival at the laboratory. The bulk samples were used for soil texture and organic matter analyses and the 0–9 cm and 9–18 cm probe samples were used for MP analyses.

### 2.3 Soil characterization & preparation

The bulk and probe samples were each passed through a 4.75 mm sieve for homogenization then dried at 50 °C overnight. This drying temperature was chosen to prevent thermal oxidization of MPs in samples. Bulk samples were sent to the Oklahoma State University Soil, Water, Forage Analytical Laboratory for texture analysis using the hydrometer method.<sup>31</sup> The organic matter content of bulk samples was determined with a loss on ignition procedure in a subset of each sample that was not used for MP analyses.<sup>32</sup> Texture and organic matter characterization and area information are provided in the ESI file (Table S1).<sup>†</sup>

### 2.4 Microplastic extraction

Microplastic extractions from the 0–9 cm and 9–18 cm soil samples of each quadrant were performed in triplicate. For each replicate, 10 g of dry soil was elutriated following the procedure outlined in Forsythe *et al.*<sup>33</sup> to remove dense non-plastic material from the sample. Briefly, 10 g of dry soil was sonicated in DI water to break up aggregates, then elutriated in a column for 15 min using an upflow velocity of 1.3 cm s<sup>-1</sup>. Particles with a lower settling velocity were captured in a 45 µm effluent collection sieve. Particles in the sieve were rinsed into a glass beaker with water for transport to the designated MP laboratory. At the MP laboratory, the water-particle slurry was filtered through a 20 µm stainless steel mesh using a glass filter unit. Particles retained on the mesh were rinsed into a 250 mL glass Erlenmeyer flask with 150 mL of 7.5% w/w NaOCl for digestion. Erlenmeyer flasks were secured on an incubator shaker table at 300 rpm at 50 °C for 24 h. After this, digestate was filtered through a 20 µm stainless steel mesh using a glass filter unit. Retained particles were thoroughly rinsed with DI water, then rinsed into 15 mL falcon tubes using 5.1 M ZnCl<sub>2</sub> ( $\sim 693$  g L<sup>-1</sup>) for a density separation procedure.<sup>34</sup> Falcon tubes were vortexed then centrifuged at  $\sim 12\,300$  ms<sup>-2</sup> for 5 min. The supernatant was filtered onto a 20 µm stainless steel mesh, and tubes were refilled with ZnCl<sub>2</sub> and vortexed until the pellet was resuspended and well-mixed. This procedure was repeated until each falcon tube had been centrifuged and the supernatant filtered three times. The particles retained from the supernatant were rinsed thoroughly with DI water, then rinsed onto a 13 mm diameter 2 µm pore size Al<sub>2</sub>O<sub>3</sub> filter for MPs analyses using a glass filtration unit.

### 2.5 Particle quantification and size analysis

The particle quantification and size analyses were performed according to Quiambao *et al.*<sup>35</sup> and details of the method are

available in the ESI.<sup>†</sup> Briefly, extracted particles were imaged with a stereomicroscope (AmScope 7X-180X Trinocular Zoom Stereo Microscope) as initial visual identification using Al<sub>2</sub>O<sub>3</sub> filters. Each Al<sub>2</sub>O<sub>3</sub> filter was placed in a clean glass Petri dish and dyed with  $\sim 30$  µL of 2 µg Nile Red per mL methanol solution for fluorescence microscopy analyses. Particles were left to react with the dye for 10 min then rinsed with 200 µL of ACS grade ethanol on a glass filtration stack to remove excess dye. Filters were placed in a Greiner 6-well plate and imaged with a fluorescence microscope (Cytation 5 Cell Imaging Multi Mode Reader, Agilent Technologies) using an RFP filter cube (excitation 531 nm/emission 593 nm). Gen5® software was used for imaging, which allowed us to obtain a single stitched image of each filter from a series of 4x magnification images (Tables S6–S9<sup>†</sup>). The resolution limit of Cytation 5 cell Imaging at this magnification is about 15 µm pixel<sup>-1</sup>. Each image was pre-processed to reduce background fluorescence. Microplastics were quantified by running the stitched image through the MPVAT 2.0 macros using ImageJ.<sup>36</sup> To avoid over-quantification caused by the 15 µm pixel<sup>-1</sup> limit of the Cytation, particles smaller than 40 µm were excluded from quantification and only the filter flow-through area was considered. Stereomicroscope and fluorescence microscope images are found in Tables S6–S9.<sup>†</sup>

### 2.6 Attenuated Total Reflectance – Fourier Transform Infrared spectroscopy analyses of MPs

The functional chemistry of suspected MPs was determined using Attenuated Total Reflectance – Fourier Transform Infrared spectroscopy (ATR-FTIR, Thermo Nicolet iN10 MX) which has a detection limit of 20 µm. One representative filter from each triplicate was selected for ATR-FTIR analysis. Ten percent of the suspected plastic particles identified during fluorescence quantification were analyzed with µ ATR-FTIR; a minimum of five particles were required for all filters regardless of MP count and a maximum cap was set at 15 particles due to lengthy analysis time. In total, 59 particles were examined from Tuttle burn site, 110 from Crow Agency burn site, and 120 from Lodge Grass dump site. Each filter was mounted on a gold mirror slide and a mosaic image of the filter flow-through area was acquired with OMNIC Picta® software to aid in the selection of particles. ATR-FTIR measurements were collected with a cooled detector and Germanium tip, 51 s collection time with 256 scans, spectral range of 4000–675 cm<sup>-1</sup> and a resolution of 8 cm<sup>-1</sup>. Aperture size was adapted to fit each examined particle. The resulting spectra were searched against the OMNIC Picta® stock polymer libraries (HR Polymer Additives and Plasticizers, Hummel Polymer Sample Library, Polymer Laminate Films, and Synthetic Fibers by Microscope) and an in-house generated library which included thermally oxidized plastic spectra described below (Table S2<sup>†</sup>). An in-house library was generated by adding the ATR spectra of common consumer plastics (bottles, wrappers, containers) which were thermally oxidized in an oven at 100, 200, and 300 °C for 1, 8, and 48 h. Prior to oxidation all materials were carefully cleaned. The library was also augmented with UV oxidized



plastics. Using the procedure by Yang *et al.*,<sup>37</sup> a particle match >70% was automatically considered plastic. A match between 60–70% required manual visual comparison against the library polymer spectrum and was interpreted based on similarities in absorption peaks. Any match under 60% was not considered a plastic.

## 2.7 Pyrolysis gas chromatography/mass spectrometry

Soil samples were prepared for Pyrolysis gas chromatography/mass spectrometry (py-GC/MS) following the methodology explained in the section 2.3 Soil Characterization and Preparation of this manuscript.<sup>33</sup> Briefly, samples were weighed out between 1–2 mg on an ultra-balance (EPE26 Precision Balance, Mettler Toledo). Analysis was conducted with an EGA/PY-3030D pyrolysis unit (Frontier Labs, Koriyama, Japan) attached to an Agilent 6890 GC/5975 MS system (Agilent, Santa Clara, CA). Quantification was performed following the method of described by Forsythe *et al.*,<sup>33</sup> and all measured masses were normalized to the original sample mass to give units of mg (plastics) to g (dry soil)<sup>-1</sup>.

## 2.8 Data analyses

All statistical analyses were performed in Minitab Statistical Software 22® and Microsoft Excel®. Outliers were determined by Grubb's test, and outliers were excluded from further analysis. All sample groups were then tested for normality using a Kolmogorov–Smirnov test. Samples from Lodge Grass, Crow Agency, and Tuttle were compared to the lab control and their corresponding background points, and differences were assessed for each site between depths and locations. One-way ANOVA and unpaired *t*-tests were performed to determine the significance of observed differences.

## 2.9 Microplastic name abbreviations

We used the following acronyms to describe the polymer types: high density polyethylene (HDPE), low density polyethylene (PE), low linear density polyethylene (LLDP), nylon 6 (N6), nylon 66 (N66), polycarbonate (PC), polyethylene (PE), polyethylene terephthalate (PET), polypropylene (PP), polyvinyl chloride (PVC), polystyrene (PS), rayon (CV).

# 3 Results and discussion

## 3.1 Open dumping and burning sites contribute to microplastic pollution

Particle abundance: both community-wide open dump and open burn sites contributed significantly ( $p < 0.05$ , Table S21†) to environmental contamination. The highest particle abundance was detected in the Lodge Grass dump site with a mean of 17 900 particles kg<sup>-1</sup> in the 0–9 cm profile and 24 000 particles kg<sup>-1</sup> in the 9–18 cm profile (Fig. 1A). In the Crow Agency site, the mean particle abundance was 14 700 particles kg<sup>-1</sup> in the 0–9 cm profile and 17 200 particles kg<sup>-1</sup> in the 9–18 cm profile. Our data also indicate that the community-wide open dumping and burning sites contained a significantly higher abundance ( $p < 0.05$ , Table S21†) of particles compared to the

single-family site (Fig. 1). At all three sites, the highest MP count was observed in the 9–18 cm soil depth though they show no significant differences ( $p$ -value 0.05, Table S21†).

The abundance of particles at the three sites is equivalent to or exceeds reported concentrations from currently understood key sources of terrestrial MPs including biosolids application and other agricultural practices.<sup>38,39</sup> For example, biosolids can contain up to 14 000 items kg<sup>-1</sup>, and concentrations higher than 5190 particles kg<sup>-1</sup> soil have been found in biosolids-applied agricultural fields.<sup>40,41</sup> A range from 900 to 40 800 items kg<sup>-1</sup> soil was found in agricultural soils in Yunnan Province, China – the abundance attributed in part to plastic mulching.<sup>42</sup> The high concentration of particles detected at the Tuttle burn site, Crow Agency burn site, and Lodge Grass dump site evidenced that open dumping and burning of solid waste are a key source of terrestrial MP pollution, especially in the rural and underserved communities that must utilize the practice.

The quantity of particles detected in each replicate (analytical replicate made from each composite) of all quadrants at Tuttle burn site, Crow Agency burn site, and Lodge Grass dump site is shown in Table S4,† respectively. Quantification at background sites and in lab controls is found in Table S5.† Stereomicroscopy and fluorescence microscopy for all sites, background, and lab controls are shown in Tables S6–S9.†

Particle size: the average size of particles found at Crow Agency site was  $228.4 \pm 136.97$  and  $226.8 \pm 117.30$   $\mu\text{m}$  for the 0–9 cm and 9–18 cm cores, respectively (Fig. 1D). At the Lodge Grass site, the average size was  $224.3 \pm 128.73$  and  $263.9 \pm 187.11$   $\mu\text{m}$  for the 0–9 cm and 9–18 cm cores, respectively (Fig. 1E). Finally, the Tuttle site contained particles with an average size of  $224.5 \pm 106.99$  and  $191.8 \pm 84.72$   $\mu\text{m}$  (Fig. 1F). The wide range of particle size (126.4–1872.8  $\mu\text{m}$ ) highlights the heterogeneity of particle sizes found in these sites. Smaller particles likely occur in these samples; however, the detection limit was restricted to 130  $\mu\text{m}$  by the high throughput of samples we analyzed.

We present differences between depths as a stratification ratio (the ratio of particles found in the upper/lower profile) and explore associations with clay content (Fig. 2). Six sites with low clay had higher abundance in the 0–9 cm depth compared with 3 sites in the 9–18 cm depth. There are a number of factors which can contribute to the migration and accumulation of MPs throughout a soil profile.<sup>43</sup> Roots and nematodes can influence the mobility of MP; for example, corn roots have contributed to the upward migration of MPs in soil depth of 6–12 cm, while earthworms influenced the transport of MPs to deeper sediments.<sup>21,44</sup> Wet and dry cycling can also contribute to the transport of MPs into the deeper soil column, with more cycling corresponding to deeper migration of MPs and smaller MPs (<21  $\mu\text{m}$ ) showing the highest mobility.<sup>45</sup> Topography, soil texture, soil compaction, organic matter, and other soil metrics may affect the transport of MPs. Additionally, freeze-thaw cycling may contribute to differences in MP transport throughout the soil profile at each site.<sup>45</sup>

In our experiments, the soil texture of the Tuttle burn site was sandy or sandy loam, while the soil sampled at Crow Agency



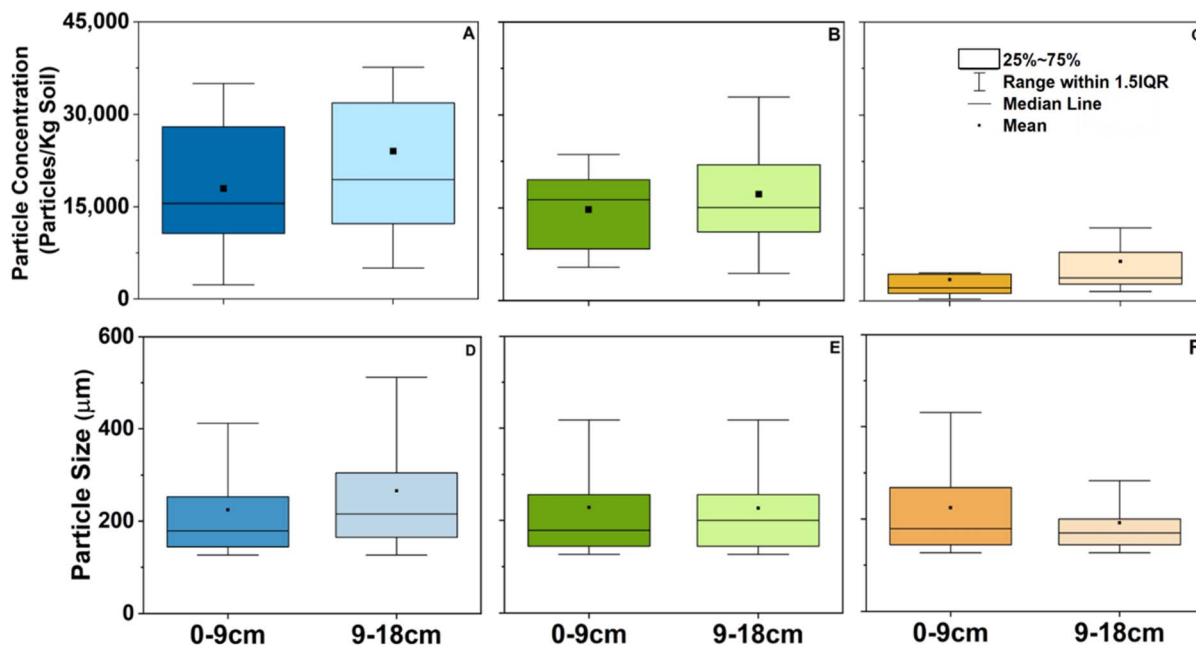


Fig. 1 Abundance of particles (particles  $\text{kg}^{-1}$  soil) at each soil depth at Lodge Grass dump site (A), Crow Agency burn site (B), and Tuttle burn site (C) and size distribution of all particles detected with Nile Red at Lodge Grass dump site (D), Crow Agency burn site (E), and Tuttle burn site (F). All analyses were performed in analytical triplicate.

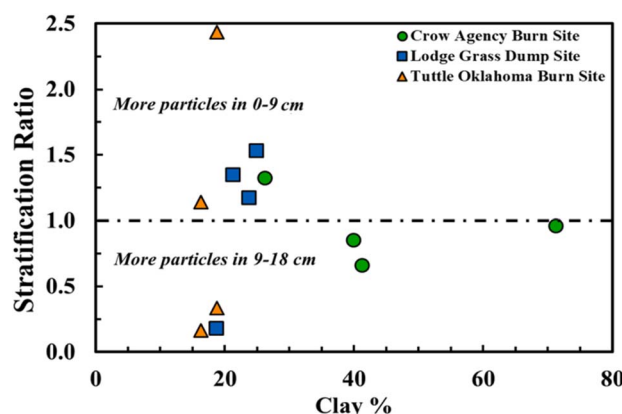


Fig. 2 Stratification ratio of particle abundance (particle concentration at 0–9 cm/particle concentration at 9–18 cm) plotted against percentage of clay in all quadrants of each site.

and Lodge Grass contained higher content of clay and may have held more water-stable aggregates. Particularly, the soil sampled in Crow Agency contained 2.5 times more clay than the Tuttle soil. Clay is often positively associated with forming aggregates and controlling pore architecture.<sup>46</sup> In soils with clay content such as Lodge Grass dump site, larger MPs could potentially infiltrate deeper into the soil due to less-compact characteristics and/or greater pore connectivity. Conversely, only smaller particles could infiltrate the highly compact soil at Tuttle burn site due to potentially decreased pore connectivity and reduced water infiltration. Clay particles are highly reactive and may affect the transport of MPs into lower depths.<sup>47</sup> The 9–18 cm profile of Crow Agency burn site contained more MPs in

three of the four quadrants; these clay-rich soils may promote the accumulation of MPs at this depth due to clay-MP interactions. There was little difference in soil texture across the quadrants of Lodge Grass dump site and Tuttle burn site (single family). Thus, the variation in stratification ratio should consider other variables alongside texture including bulk density, aggregation, and water infiltration.

The few studies have examined the vertical distribution of MPs through the terrestrial soil environment have found contrasting results.<sup>40,48,49</sup> For example, MP abundance was slightly higher at 20 cm depth (mean particle concentration = 53.2 items  $\text{m}^{-2}$ ) compared to 5 cm depth (mean particle concentration = 34.6 items  $\text{m}^{-2}$ ), and smaller average particle size was observed in the deeper profiles in agricultural soils from China.<sup>48</sup> A 3-times higher concentration in the 0–10 cm profile compared to the 20–30 cm was quantified in German agricultural fields.<sup>49</sup> Microplastics concentrations did not significantly vary between 0–10 cm and 10–30 cm soil depths of biosolids-applied fields in Spain.<sup>40</sup> These results and our data indicate that it is not possible to make generalizations about the distribution of MPs through the soil profile.

### 3.2 Functional chemistry analysis of MP

A total of 58 of the 60 particles examined from Tuttle burn site, 105 of 110 particles examined from Crow Agency burn site, and 118 of 120 particles examined from Lodge Grass dump site were confirmed as MPs by ATR-FTIR. Almost all MPs identified at each site matched with burned or UV aged plastic spectra. Examples of identified MPs from each site are shown in Fig. 3 and all examined particles are shown in Tables S10–S16 and S21.† Oxidation features or changes in the spectra can be



observed in several particles compared to the reference spectra (Fig. 3A–F). The spectra were analyzed according to the correlation charts described in Larkin *et al.*<sup>50</sup> The functional chemistry of LLDPE MPs indicated changes in the alkane C–H stretching region (3000–2840  $\text{cm}^{-1}$ ),  $\text{sp}^3$  C–H bend (~1410–1325  $\text{cm}^{-1}$ ), C–O (1125–1000  $\text{cm}^{-1}$ ), and alkene  $\text{sp}^2$  C–H (650–1000  $\text{cm}^{-1}$ ) compared to the reference spectrum (Fig. 3A).

Likewise, the functional chemistry of PE shifted in the alkane C–H stretching region (3000–2840  $\text{cm}^{-1}$ ),  $\text{sp}^3$  C–H bend (~1410–1325  $\text{cm}^{-1}$ ), C–O (1125–1000  $\text{cm}^{-1}$ ), and alkene  $\text{sp}^2$  C–H (1000–650  $\text{cm}^{-1}$ ) and PP MPs (Fig. 3A–C). On the other hand, PS MPs show different features in the aromatic C=C-stretching region (1675–1475  $\text{cm}^{-1}$ ) (Fig. 3D–F). Our results indicate that in open burning sites, MPs are exposed to conditions that modify their functional chemistry which likely affects the reactivity and mobility of those MPs in the environment.

Discrepancy in the functional chemistry of the reference spectra, environmentally weathered MPs, and thermally oxidized MPs likely leads to the misidentification or under-identification of microplastics by current spectral identification tools. The current challenges of spectral identification

highlight the need to generate more environmentally relevant spectral libraries that contain thermally aged polymers. However, more information is needed regarding the occurrence of thermally oxidized MPs in the environment.

High temperatures and UV radiation may be both defined as oxidation processes; however, UV radiation is driven by photochemical reactions (*e.g.*, oxidation, reduction decomposition, and polymerization).<sup>51</sup> Particularly in thicker plastics, these are diffusion dependent and occur in the first 500 to 900  $\mu\text{m}$  layer of the plastic.<sup>52</sup> Thermal oxidation, on the other hand, can affect the surface and bulk within the same process as a function of the temperature regardless of the thickness of the plastic.

Both high temperatures and UV radiation cause oxidation, but through different mechanisms.<sup>53</sup> Although both processes produce the similar functional groups, differences in the mechanisms that produce these functional groups can lead to mischaracterization if reference libraries lack a wide array of spectra. In our study, to analyze the effects of UV and thermal oxidation, we compared the specific changes in the functional groups of PE and PS under these conditions (Fig. 4). Our data show that UV radiation induced less oxidation in the PE

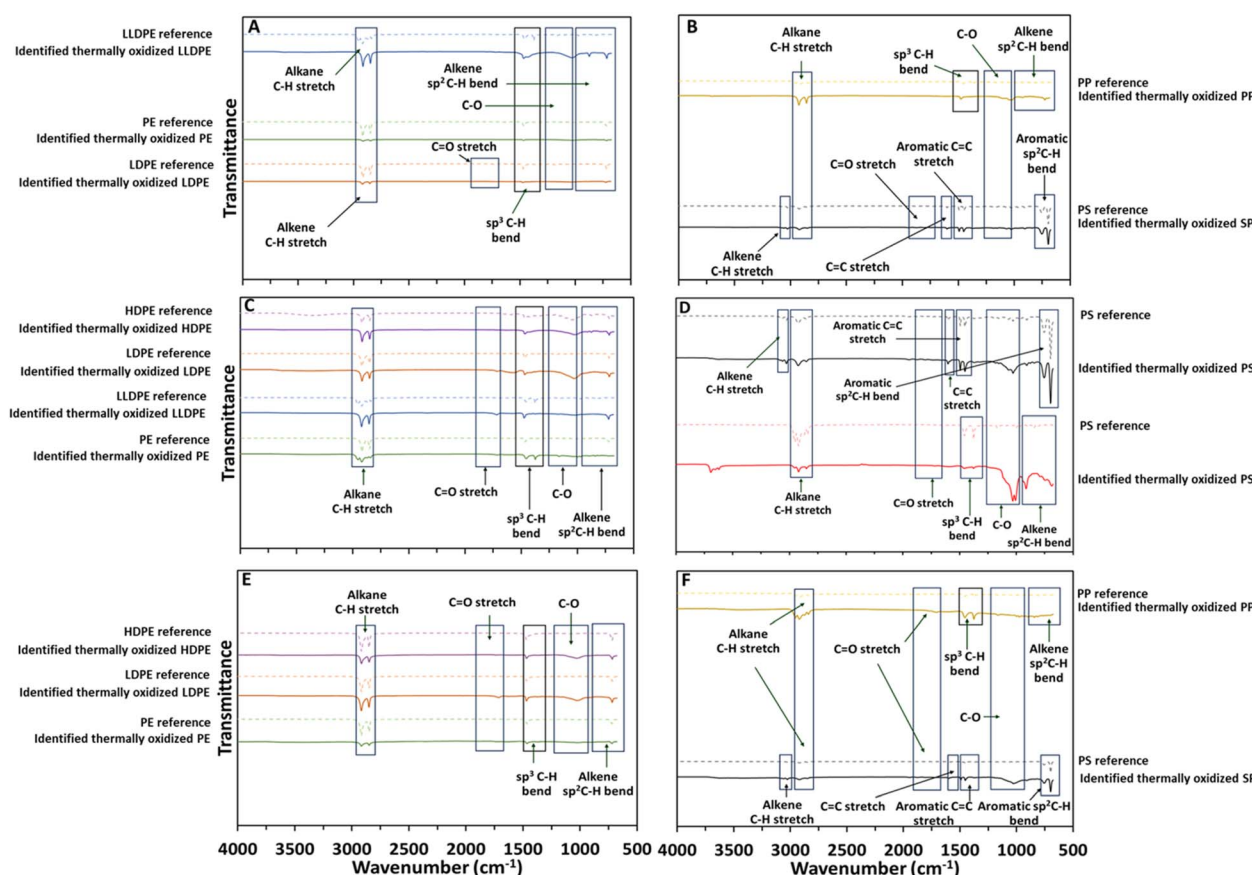


Fig. 3 Comparison of representative FTIR spectra of selected MPs found open dumping and burning sites respect to the plastic reference of polyethylene-containing MPs (A–C) and other prevalent types of MPs (D–F). Particles shown in panel A are CABS-NW-Shallow-1 (LLDPE), CABS-NE-Shallow-5 (PE), CABS-NW-Deep-3 (LDPE). Particles shown in panel B: LG-NW-Shallow-1 (HDPE), LG-NW-Deep-4 (LLDPE), LG-W-Deep-5 (PE), LG-SW-Deep-2 (LDPE). Particles shown in panel C: Tuttle OK-West-Shallow-1 (HDPE), Tuttle OK North-Shallow-3 (PE), Tuttle OK-West-Deep-3 (LDPE). Particles shown in panel D: CABS-NE-Shallow-3 (PP), CABS-SE-Deep-1. Particles shown in panel E: LG-SW-Shallow-1 (PS). Particles shown in panel F are Tuttle OK-East-Shallow-2 (PS), Tuttle OK-East-Deep-3 (PP). The information for the rest of the particles is available in the ESI† File.



functional chemistry (Fig. 5a). The lack of chromophore species in PE results in non-UV absorbing structure. Functional groups observed in the spectrum are likely linked to unidentified chromophores from additives that absorb UV light and generate radicals, leading to ketones ( $1712\text{ cm}^{-1}$ ) and vinyl-type unsaturation ( $909\text{ cm}^{-1}$ ,  $987\text{ cm}^{-1}$ ,  $\sim 1640\text{ cm}^{-1}$ ) which is consistent with previous research.<sup>51,53,54</sup> In contrast, thermal oxidation caused the loss of characteristic peaks (2926, 2855, 1465, 1465, and  $720\text{ cm}^{-1}$ ) along with the formation of radicals ( $1369\text{ cm}^{-1}$  and  $1407\text{ cm}^{-1}$ ) and carbonyl groups ( $1712\text{ cm}^{-1}$ ,  $1180\text{ cm}^{-1}$ , and  $1018\text{ cm}^{-1}$ ), respectively. These observations agreed with previous findings which found similar effects on the functional chemistry of PE.<sup>53,54</sup> Previous studies have found that at temperatures above  $300\text{ }^{\circ}\text{C}$ ,  $\text{C}=\text{C}$  stretching may be caused by dehydrogenation of an alkane, resulting from the material degradation and increasing temperatures.<sup>54</sup>

Polystyrene, unlike PE, contains chromophores in its structure (specifically the phenyl ring), which makes it easier to identify the distinct effects of UV compared to thermal oxidation (Fig. 5B).<sup>51</sup> Data indicate that UV exposure decreased the characteristic peaks at  $2919\text{ cm}^{-1}$  and generated  $\text{C}=\text{O}$  stretching groups ( $1727\text{ cm}^{-1}$ ), while thermal oxidation generated  $\text{C}=\text{O}$  stretch at  $1680\text{ cm}^{-1}$ . However, we observed no other clear differences between these oxidation processes. These results suggest that chromophores in polymers induce a more efficient absorption of UV radiation at a wider wavelength which results in a broader attack on the functional chemistry of the polymer. Other studies that have explored PS degradation UV conditions also suggest that the chromophore of PS (*i.e.*, the phenyl functional group) plays a role absorbing UV radiation.<sup>55</sup> On the other hand, thermal oxidation decreased the signal of the peaks at  $1600$ ,  $1500$  and  $1468\text{ cm}^{-1}$ .<sup>56</sup> Our work evidenced that open dumping and burning of solid wastes are a source of MPs with a distinct functional chemical signature.

### 3.3 Thermally oxidized MPs in soils nearby open burning sites

Our results indicated that burned MPs occurred with more frequency in all the sites across the different depths (Fig. 5). In

the 0–9 cm depth, the prevalence of burned MPs ranged from 71.2% to 89.8% (Fig. 5A), while the prevalence of burned MPs of the 9–18 cm depth ranged from 82.1% to 93.8% across the three sites (Fig. 5A). Lodge Grass, MT, was the site with the highest abundance of burned MPs in the 0–9 cm range (89.8%), while Tuttle, OK, was the site with highest relative abundance in the 9–18 cm range (93.8%). In all the sites, polyethylene-bearing burned MPs (*i.e.*, HDPE, LDPE, LLDPE) showed the highest abundance in both soil depths across all sites (34.6–76.3%). Finally, when considering the abundance of all plastics regardless of their state of oxidation, polyethylene-bearing MPs were the most abundant type in all depths and sites (average  $69.78\% \pm 14.61$ ), followed by PP ( $8.27\% \pm 7.88$ ), CV( $6.41\% \pm 4.29$ ), and PS ( $5.62\% \pm 3.85$ ).

The higher prevalence of PE compared to other polymers was confirmed by py-GC/MS in all the sites sampled for total depths reported (Crow Agency burn site at  $5.97 \pm 1.75\text{ mg g}^{-1}$ , Lodge Grass dump site at  $4.99 \pm 1.95\text{ mg g}^{-1}$ , and Tuttle burn site at  $6.13 \pm 2.59\text{ mg g}^{-1}$ ) (Fig. 6). These data show very similar concentrations of microplastics across sites including the single-family site. However, the actual concentration of MPs found in these samples with py-GC/MS may be underestimated since the reference materials (standards) available for making calibration curves and quantifying MPs exclude thermally and UV oxidized MPs. Microplastics were found with less frequency at background locations and lab controls than at the open dump and burn sites.

No discernible pattern can be observed in the polymer type as a function of depth. For instance, the abundance of PE was dominant across five data sets, but we did not detect PE in the 9–18 cm depth from the Tuttle, OK site. From the Crow Agency site, we did not detect any other polymer in 9–18 cm depth, while Lodge Grass showed a greater diversity of synthetic polymer in the 9–18 cm depth.

Only two MPs were detected from the representative lab control sample: one polyethylene and one polypropylene, likely from laboratory procedures in which plastic could not be avoided. Compared to lab controls and background site particles which were primarily white or clear fibers, a variety of particle

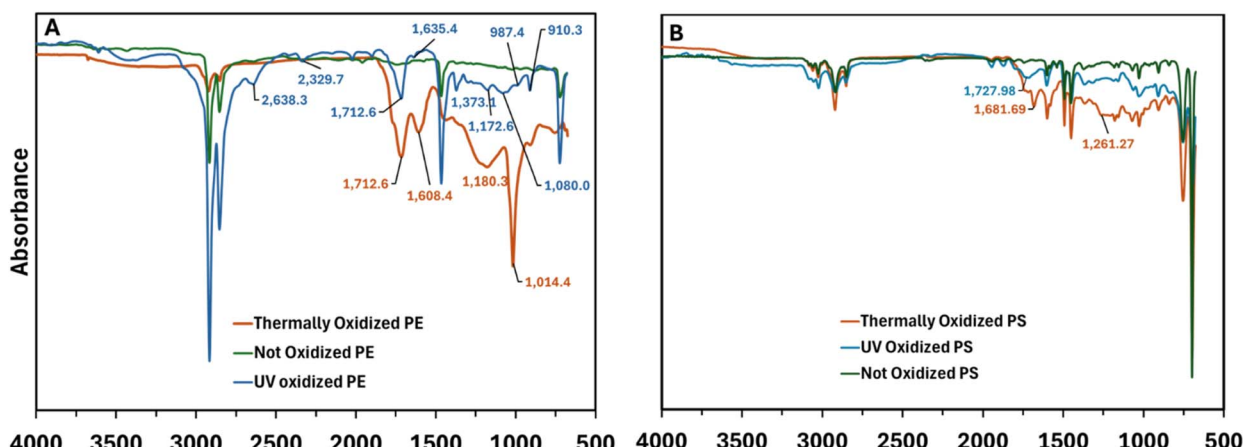


Fig. 4 Effects of thermal and UV oxidation on the functional chemistry of PE and PS microplastics.



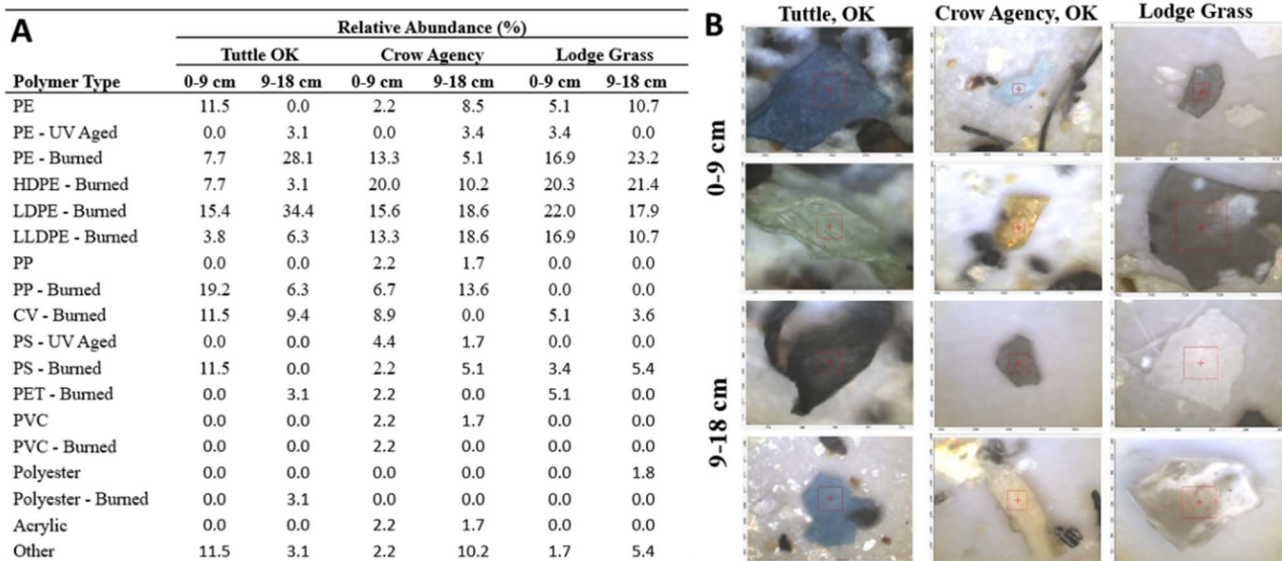


Fig. 5 Microplastics found in the sites sampled. (A) Relative abundance. (B) Representative microplastics found in the sites of Tuttle OK (top to bottom): Tuttle OK-West-Shallow-1, Tuttle OK-W-Deep-1 Tuttle OK-W-Deep-2, Tuttle OK-W-Deep-7; microplastics found in Crow Agency (top to bottom): CABS-NW Shallow-2, CABS-NW-Shallow-12 CABS-SE-Deep-4; and microplastics found in Lodge Grass: LG-SW-Deep-12; LG-SW-Shallow-13; LG-SW-Shallow-7. CABS: Crow Agency burn site; LG: Lodge Grass. N, S, W, E indicate cardinal directions.

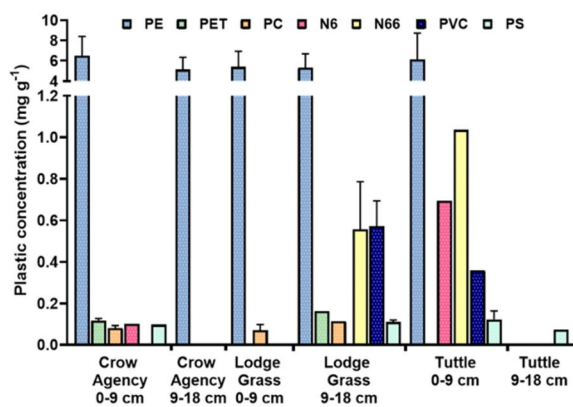
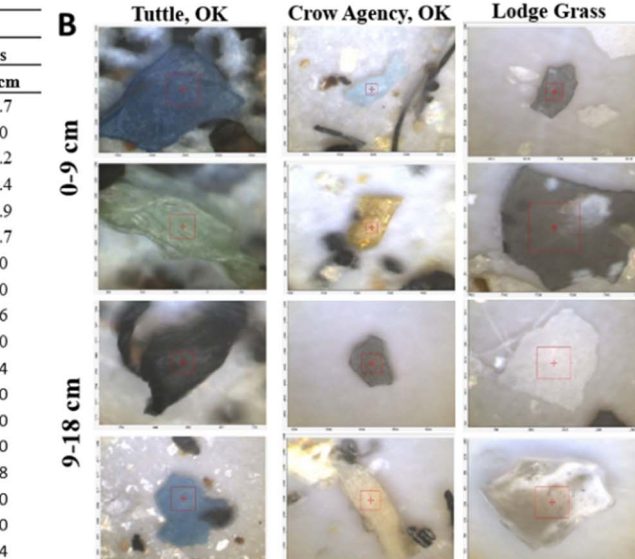


Fig. 6 Soil plastic concentration ( $\text{mg g}^{-1}$ ) measured by py-GC/MS for the Crow Agency burn site, Lodge Grass dump site, and Tuttle, Oklahoma burn site 0-9 and 9-18 cm samples. Plastic types are indicated as polyethylene (PE), polyethylene terephthalate (PET), polycarbonate (PC), nylon 6 (N6), nylon 66 (N66), polyvinyl chloride (PVC), and polystyrene (PS).

morphologies (rectangular, oval-shaped, round, *etc.*) and colors (blue, pink, grey, *etc.*) were observed in the open dump and burn site particles (Fig. 5B). Overall, these findings coincide with the polymers most commonly used in household and single-use plastic products that are often discarded in municipal solid waste.<sup>57</sup>

## 4 Conclusions

The results of this work identify open dumping and burning of solid wastes as a source of elevated concentrations of terrestrial MPs. Burning practices result in the generation of oxidized MPs.



which differ in abundance, size, and functional chemistry from parent plastic waste solids. The concentration of particles found at community-wide sites equals or exceeds the concentration of potential MPs found at other sites with high concentrations of MPs. We found no significant differences in the concentration of particles across soil depths. The high concentration of MPs identified at the single-family open dumping and burning of solid waste is an issue concerning not only our partner communities for this study in Oklahoma and Montana, but also has profound global environmental implications for rural and urban underserved communities. Open dumping and burning of solid waste are utilized by approximately a quarter of all humans on earth, and more work is needed to understand the full scope and impact of this practice on the surrounding environment.

## Data availability

The data supporting this article have been included as part of the ESI.<sup>†</sup>

## Author contributions

Kendra Z. Hess: methodology, validation, formal analysis, investigation, writing – original draft, and visualization; Kyle R. Forsythe: methodology, investigation, formal analyses; Xuewen Wang: methodology, validation, investigation, formal analyses, data visualization; Andrea Arredondo-Navarro: investigation, formal analyses, data visualization; Gwen Tipling: investigation; Jesse Jones: investigation; Melissa Mata: investigation; Victoria

Hughes: investigation; Christine Martin: resources; John Doyle: resources; Justin Scott: methodology, validation, formal analysis; Matteo Minghetti: methodology, resources, writing – review and editing; Andrea Jilling: methodology, formal analyses, resources, writing – review and editing, data visualization; José M. Cerrato: resources, funding acquisition, writing – review and editing, data visualization; Eliane El Hayek: resources, funding acquisition, writing – review and editing; and Jorge Gonzalez-Estrella: conceptualization, methodology, writing – review & editing, supervision, resources, project administration, funding acquisition, data visualization.

## Conflicts of interest

There are no conflicts to declare.

## Acknowledgements

This study was funded by the National Institute on Minority Health and Health Disparities (Award Number P50MD015706), the U.S. Geological Survey (Grant/Cooperative Agreement G21AP10597), and the National Science Foundation (Award Number CAREER 2338225). Justin Scott was supported by the National Institute of Environmental Health Sciences (Award Number: 1R15ES034901-01). The content is solely the responsibility of the authors and does not necessarily represent the official views of the National Institutes of Health, the U.S. Geological Survey, nor the National Science Foundation.

## References

- 1 S. Kaza, L. C. Yao, P. Bhada-Tata and F. Van Woerden, *What a Waste 2.0 : A Global Snapshot of Solid Waste Management to 2050*, World Bank, Washington D.C., 2018.
- 2 U. EPA, *Advancing Sustainable Materials Management: Facts and Figures Report*, Environmental Protection Agency, 2020.
- 3 C. A. Velis and E. Cook, Mismanagement of Plastic Waste through Open Burning with Emphasis on the Global South: A Systematic Review of Risks to Occupational and Public Health, *Environ. Sci. Technol.*, 2021, **55**, 7186–7207.
- 4 G. Pathak, M. Nicther, A. Hardon and E. Moyer, The Open Burning of Plastic Wastes is an Urgent Global Health Issue, *Ann. Glob. Health*, 2024, **90**, 3.
- 5 W. W. Y. Lau, Y. Shiran, R. M. Bailey, E. Cook, M. R. Stuchtey, J. Koskella, C. A. Velis, L. Godfrey, J. Boucher, M. B. Murphy, R. C. Thompson, E. Jankowska, A. Castillo Castillo, T. D. Pilditch, B. Dixon, L. Koerselman, E. Kosior, E. Favoino, J. Gutberlet, S. Baulch, M. E. Atreya, D. Fischer, K. K. He, M. M. Petit, U. R. Sumaila, E. Neil, M. V. Bernhofen, K. Lawrence and J. E. Palardy, Evaluating scenarios toward zero plastic pollution, *Science*, 2020, **369**, 1455–1461.
- 6 U. S. EPA, *Biosolids Technology Fact Sheet Use of Landfilling for Biosolids Management*, 2003.
- 7 K. Rogers, E. WaMaina, A. Barber, S. Masood, C. Love, Y. H. Kim, M. I. Gilmour and I. Jaspers, Emissions from plastic incineration induce inflammation, oxidative stress, and impaired bioenergetics in primary human respiratory epithelial cells, *Toxicol. Sci.*, 2024, **199**, 301–315.
- 8 R. C. Thompson, Y. Olsen, R. P. Mitchell, A. Davis, S. J. Rowland, A. W. John, D. McGonigle and A. E. Russell, Lost at sea: where is all the plastic?, *Science*, 2004, **304**, 838.
- 9 E. El Hayek, E. Castillo, J. G. In, M. Garcia, J. Cerrato, A. Brearley, J. Gonzalez-Estrella, G. Herbert, B. Bleske, A. Benavidez, H. Hsiao, L. Yin, M. J. Campen and X. Yu, Photoaging of polystyrene microspheres causes oxidative alterations to surface physicochemistry and enhances airway epithelial toxicity, *Toxicol. Sci.*, 2023, **193**, 90–102.
- 10 E. P. Pinto, J. Scott, K. Hess, E. Paredes, J. Bellas, J. Gonzalez-Estrella and M. Minghetti, Role of UV radiation and oxidation on polyethylene micro- and nanoplastics: impacts on cadmium sorption, bioaccumulation, and toxicity in fish intestinal cells, *Environ. Sci. Pollut. Res.*, 2024, **31**, 47974–47990.
- 11 C. Miller, A. Neidhart, K. Hess, A.-M. S. Ali, A. Benavidez, M. Spilde, E. Peterson, A. Brearley, X. Wang, B. D. Dhanapala, J. M. Cerrato, J. Gonzalez-Estrella and E. El Hayek, Uranium accumulation in environmentally relevant nanoplastics and agricultural soil at acidic and circumneutral pH, *Sci. Total Environ.*, 2024, **926**, 171834.
- 12 Y. K. Song, S. H. Hong, M. Jang, G. M. Han, S. W. Jung and W. J. Shim, Combined Effects of UV Exposure Duration and Mechanical Abrasion on Microplastic Fragmentation by Polymer Type, *Environ. Sci. Technol.*, 2017, **51**, 4368–4376.
- 13 V. Fauvelle, M. Garel, C. Tamburini, D. Nerini, J. Castro-Jiménez, N. Schmidt, A. Paluselli, A. Fahs, L. Papillon, A. M. Booth and R. Sempéré, Organic additive release from plastic to seawater is lower under deep-sea conditions, *Nat. Commun.*, 2021, **12**, 4426.
- 14 A. Paluselli, V. Fauvelle, F. Galgani and R. Sempéré, Phthalate Release from Plastic Fragments and Degradation in Seawater, *Environ. Sci. Technol.*, 2019, **53**, 166–175.
- 15 L. Hu, J. Fu, S. Wang, Y. Xiang and X. Pan, Microplastics generated under simulated fire scenarios: Characteristics, antimony leaching, and toxicity, *Environ. Pollut.*, 2021, **269**, 115905.
- 16 P. K. Rai, C. Sonne, R. J. C. Brown, S. A. Younis and K.-H. Kim, Adsorption of environmental contaminants on micro- and nano-scale plastic polymers and the influence of weathering processes on their adsorptive attributes, *J. Hazard. Mater.*, 2022, **427**, 127903.
- 17 Y. Xu, Q. Ou, J. P. van der Hoek, G. Liu and K. M. Lompe, Photo-oxidation of Micro- and Nanoplastics: Physical, Chemical, and Biological Effects in Environments, *Environ. Sci. Technol.*, 2024, **58**, 991–1009.
- 18 D. He, Y. Luo, S. Lu, M. Liu, Y. Song and L. Lei, Microplastics in soils: Analytical methods, pollution characteristics and ecological risks, *TrAC, Trends Anal. Chem.*, 2018, **109**, 163–172.
- 19 A. A. De Souza MacHado, C. W. Lau, J. Till, W. Klosas, A. Lehmann, R. Becker and M. C. Rillig, Impacts of Microplastics on the Soil Biophysical Environment, *Environ. Sci. Technol.*, 2018, **52**, 9656–9665.



20 M. C. Rillig, S. W. Kim and Y.-G. Zhu, The soil plastisphere, *Nat. Rev. Microbiol.*, 2024, **22**, 64–74.

21 M. C. Rillig, L. Ziersch and S. Hempel, Microplastic transport in soil by earthworms, *Sci. Rep.*, 2017, **7**, 1362.

22 K. Duis and A. Coors, Microplastics in the aquatic and terrestrial environment: sources (with a specific focus on personal care products), fate and effects, *Environ. Sci.*, 2016, **28**, 2.

23 J. Lei, X. Zhang, W. Yan, X. Chen, Z. Li, P. Dan, Q. Dan, W. Jiang, Q. Liu and Y. Li, Urban Microplastic Pollution Revealed by a Large-Scale Wetland Soil Survey, *Environ. Sci. Technol.*, 2023, **57**, 8035–8043.

24 G. Hamer, Solid waste treatment and disposal: effects on public health and environmental safety, *Biotechnol. Adv.*, 2003, **22**, 71–79.

25 N. Ferronato and V. Torretta, Waste Mismanagement in Developing Countries: A Review of Global Issues, *Int. J. Environ. Res. Public Health*, 2019, **16**, 1060.

26 N. Kováts, K. Hubai, T.-A. Sainnokhoin, B. Eck-Varanka, A. Hoffer, Á. Tóth, B. Kakasi and G. Teke, Ecotoxic emissions generated by illegal burning of household waste, *Chemosphere*, 2022, **298**, 134263.

27 G. Pathak, M. Nicther, A. Hardon, E. Moyer, A. Latkar, J. Simbaya, D. Pakasi, E. Taqueban and J. Love, Plastic pollution and the open burning of plastic wastes, *Glob. Environ. Change*, 2023, **80**, 102648.

28 Y. Su, Z. Zhang, D. Wu, L. Zhan, H. Shi and B. Xie, Occurrence of microplastics in landfill systems and their fate with landfill age, *Water Res.*, 2019, **164**, 114968.

29 H. Golwala, X. Zhang, S. M. Iskander and A. L. Smith, Solid waste: An overlooked source of microplastics to the environment, *Sci. Total Environ.*, 2021, **769**, 144581.

30 M. Kazour, S. Terki, K. Rabhi, S. Jemaa, G. Khalaf and R. Amara, Sources of microplastics pollution in the marine environment: Importance of wastewater treatment plant and coastal landfill, *Mar. Pollut. Bull.*, 2019, **146**, 608–618.

31 A. Klute, *Methods of Soil Analysis. Part 1*, American Society of Agronomy, Inc. Publishes, Madison, Wisconsin, USA, 2nd edn, 1986.

32 M. R. Carter and E. G. Gregorich, *Soil Sampling and Methods of Analysis*, CRC press, 2007.

33 K. Forsythe, M. Egermeier, M. Garcia, R. Liu, M. Campen, M. Minghetti, A. Jilling and J. Gonzalez-Estrella, Viability of elutriation for the extraction of microplastics from environmental soil samples, *Environ. Sci.: Adv.*, 2024, **3**, 1039–1047.

34 S. S. Monteiro, T. Rocha-Santos, J. C. Prata, A. C. Duarte, A. V. Girão, P. Lopes, T. Cristovão and J. P. da Costa, A straightforward method for microplastic extraction from organic-rich freshwater samples, *Sci. Total Environ.*, 2022, **815**, 152941.

35 J. Quiambao, K. Z. Hess, S. Johnston, E. El Hayek, A. Noureddine, A.-M. S. Ali, M. Spilde, A. Brearley, P. Lichtner, J. M. Cerrato, K. J. Howe and J. Gonzalez-Estrella, Interfacial Interactions of Uranium and Arsenic with Microplastics: From Field Detection to Controlled Laboratory Tests, *Environ. Eng. Sci.*, 2023, **40**, 562–573.

36 J. C. Prata, J. R. Alves, J. P. da Costa, A. C. Duarte and T. Rocha-Santos, Major factors influencing the quantification of Nile Red stained microplastics and improved automatic quantification (MP-VAT 2.0), *Sci. Total Environ.*, 2020, **719**, 137498.

37 D. Yang, H. Shi, L. Li, J. Li, K. Jabeen and P. Kolandhasamy, Microplastic Pollution in Table Salts from China, *Environ. Sci. Technol.*, 2015, **49**, 13622–13627.

38 T. Jin, J. Tang, H. Lyu, L. Wang, A. B. Gillmore and S. M. Schaeffer, Activities of Microplastics (MPs) in Agricultural Soil: A Review of MPs Pollution from the Perspective of Agricultural Ecosystems, *J. Agric. Food Chem.*, 2022, **70**, 4182–4201.

39 H. Liu, Z. Wang, L. D. Nghiem, L. Gao, A. Zamyadi, Z. Zhang, J. Sun and Q. Wang, Solid-Embedded Microplastics from Sewage Sludge to Agricultural Soils: Detection, Occurrence, and Impacts, *ACS ES&T Water*, 2021, **1**, 1322–1333.

40 P. van den Berg, E. Huerta-Lwanga, F. Corradini and V. Geissen, Sewage sludge application as a vehicle for microplastics in eastern Spanish agricultural soils, *Environ. Pollut.*, 2020, **261**, 114198.

41 J. Crossman, R. R. Hurley, M. Futter and L. Nizzetto, Transfer and transport of microplastics from biosolids to agricultural soils and the wider environment, *Sci. Total Environ.*, 2020, **724**, 138334.

42 Y. Huang, Q. Liu, W. Jia, C. Yan and J. Wang, Agricultural plastic mulching as a source of microplastics in the terrestrial environment, *Environ. Pollut.*, 2020, **260**, 114096.

43 J.-J. Guo, X.-P. Huang, L. Xiang, Y.-Z. Wang, Y.-W. Li, H. Li, Q.-Y. Cai, C.-H. Mo and M.-H. Wong, Source, migration and toxicology of microplastics in soil, *Environ. Int.*, 2020, **137**, 105263.

44 H. Li, X. Lu, S. Wang, B. Zheng and Y. Xu, Vertical migration of microplastics along soil profile under different crop root systems, *Environ. Pollut.*, 2021, **278**, 116833.

45 D. O'Connor, S. Pan, Z. Shen, Y. Song, Y. Jin, W.-M. Wu and D. Hou, Microplastics undergo accelerated vertical migration in sand soil due to small size and wet-dry cycles, *Environ. Pollut.*, 2019, **249**, 527–534.

46 G. Adhikari and K. G. Bhattacharyya, Correlation of soil organic carbon and nutrients (NPK) to soil mineralogy, texture, aggregation, and land use pattern, *Environ. Monit. Assess.*, 2015, **187**, 735.

47 P. H. Nadeau, The physical dimensions of fundamental clay particles, *Clay Miner.*, 1985, **20**, 499–514.

48 H. Fakour, S.-L. Lo, N. T. Yoashi, A. M. Massao, N. N. Lema, F. B. Mkhontfo, P. C. Jomalema, N. S. Jumanne, B. H. Mbuya, J. T. Mtweve and M. Imani, Quantification and Analysis of Microplastics in Farmland Soils: Characterization, Sources, and Pathways, *Agriculture*, 2021, **11**.

49 I. K. Harms, T. Diekötter, S. Troegel and M. Lenz, Amount, distribution and composition of large microplastics in typical agricultural soils in Northern Germany, *Sci. Total Environ.*, 2021, **758**, 143615.

50 *Infrared and Raman Spectroscopy*, ed. P. J. Larkin, Elsevier, 2nd edn, 2018, pp. 261–263, DOI: [10.1016/B978-0-12-804162-8.15001-3](https://doi.org/10.1016/B978-0-12-804162-8.15001-3).



51 J. Izdebska, in *Printing on Polymers*, eds. J. Izdebska and S. Thomas, William Andrew Publishing, 2016, pp. 353–370, DOI: [10.1016/B978-0-323-37468-2.00022-1](https://doi.org/10.1016/B978-0-323-37468-2.00022-1).

52 A. L. Andrade, P. W. Barnes, J. F. Bornman, T. Gouin, S. Madronich, C. C. White, R. G. Zepp and M. A. K. Jansen, Oxidation and fragmentation of plastics in a changing environment; from UV-radiation to biological degradation, *Sci. Total Environ.*, 2022, **851**, 158022.

53 M. Gardette, A. Perthue, J.-L. Gardette, T. Janecska, E. Földes, B. Pukánszky and S. Therias, Photo- and thermal-oxidation of polyethylene: Comparison of mechanisms and influence of unsaturation content, *Polym. Degrad. Stab.*, 2013, **98**, 2383–2390.

54 B. Suresh, S. Maruthamuthu, A. Khare, N. Palanisamy, V. S. Muralidharan, R. Ragunathan, M. Kannan and K. N. Pandiyaraj, Influence of thermal oxidation on surface and thermo-mechanical properties of polyethylene, *J. Polym. Res.*, 2011, **18**, 2175–2184.

55 E. Yousif and R. Haddad, Photodegradation and photostabilization of polymers, especially polystyrene: review, *SpringerPlus*, 2013, **2**, 398.

56 B.-l. Denq, W.-y. Chiu, L.-w. Chen and C.-y. Lee, Thermal degradation behavior of polystyrene blended with propyl ester phosphazene, *Polym. Degrad. Stab.*, 1997, **57**, 261–268.

57 R. Palos, A. Gutierrez, F. J. Vela, M. Olazar, J. M. Arandes and J. Bilbao, Waste Refinery: The Valorization of Waste Plastics and End-of-Life Tires in Refinery Units. A Review, *Energy Fuels*, 2021, **35**, 3529–3557.

